

Decentralized Multi-target Tracking with Multiple Quadrotors using a PHD Filter

Aniket Shirsat* and Spring Berman.†
Arizona State University, Tempe, AZ 85287

We consider a scenario in which a group of quadrotors is tasked at tracking multiple stationary targets in an unknown, bounded environment. The quadrotors search for targets along a spatial grid overlaid on the environment while performing a random walk on this grid modeled by a discrete-time discrete-state (DTDS) Markov chain. The quadrotors can transmit their estimates of the target locations to other quadrotors that occupy their current location on the grid; thus, their communication network is time-varying and not necessarily connected. We model the search procedure as a renewal-reward process on the underlying DTDS Markov chain. To accommodate changes in the set of targets observed by each quadrotor as it explores the environment, along with uncertainties in the quadrotors' measurements of the targets, we formulate the tracking problem in terms of Random Finite Sets (RFS). The quadrotors use RFS-based Probability Hypothesis Density (PHD) filters to estimate the number of targets and their locations. We present a theoretical estimation framework, based on the Gaussian Mixture formulation of the PHD filter, and preliminary simulation results toward extending existing approaches for RFS-based multi-target tracking to a decentralized multi-robot strategy for multi-target tracking. We validate this approach with simulations of multi-target tracking scenarios with different densities of robots and targets, and we evaluate the average time required for the robots in each scenario to reach agreement on a common set of targets.

I. Introduction

Mobile ground robots [1] and aerial robots [2] have often been used for exploration and mapping tasks. Heterogeneous teams of ground and aerial robots have been employed for applications that involve mapping an environment, such as disaster response [3, 4] and surveillance [5]. Such tasks require the robots to track features of interest that are present in the environment. Mobile robots, especially quadrotors, are subject to limitations on their operation due to constraints on the payloads that they can carry, including power, sensing and communication devices for transmitting information to other robots and/or to a command center. Many multi-robot control strategies rely on a centralized communication network for coordination. For example, some multi-robot exploration strategies, e.g. [6], rely on constant two-way communication between the robots and a central node. Since a centralized communication architecture is required, these strategies do not scale well with the robot population size, as the communication bandwidth becomes a bottleneck with increasing numbers of robots. Moreover, a failure of the central node causes loss of communication for all the robots. Decentralized multi-robot control strategies can be used to overcome these limitations. Such strategies involve only local communication between robots and scale well with the number of robots. However, communication among robots can become unreliable as the number of robots increases [7], and the communication network connectivity may be disrupted by the environment [8] or by the movement of robots beyond communication range.

Multi-target tracking is an established field of research with origins in the study of point processes [9], with most early applications in radar and sonar based tracking. In real-world scenarios, there is often uncertainty in the existence, locations, and dynamics of targets, as well as uncertainty in sensor measurements of targets that arise from sensor noise and false detections (clutter) around the real targets. Random Finite Set (RFS) models provide a probabilistic framework for multi-target tracking that can account for these uncertainties and ensure statistical guarantees on the accuracy of the estimated number of targets and their states. Unlike RFS-based estimators, many classical probabilistic multi-target tracking approaches require techniques for data association, which is computationally intensive. Such approaches include multiple hypothesis tracking [10, 11], in which an exhaustive search on all possible combinations of tracks and data associations is performed, and joint probabilistic data association [12, 13]. The papers [14–16] are foundational works on estimation methods based on Random Finite Sets, and they have made concepts from

*Ph.D. student, Mechanical and Aerospace Engineering, Arizona State University, Tempe, AZ 85287.

†Associate Professor, Mechanical and Aerospace Engineering, Arizona State University, Tempe, AZ 85287.

Random Finite Set formulation and its first-order moment, the Probability Hypothesis Density (PHD) filter, as an estimation framework for detecting and tracking multiple targets. In Section V.A, we describe the Gaussian Mixture approximation of the PHD filter from [18]. We then validate our strategy with simulations in Section VI and finally state our conclusions and future work in Section VII.

II. Problem Formulation

We consider an unknown, bounded environment that contains a finite, non-zero number of static targets, indexed by the set $\mathcal{I} \subset \mathbb{Z}_+$. The environment is discretized into a square grid, and the four vertices of each grid cell are referred to as *nodes*. Let $\mathcal{S} \subset \mathbb{Z}_+$ denote the set of S nodes, and let $\mathcal{G}_s = (\mathcal{V}_s, \mathcal{E}_s)$ be an undirected graph associated with this grid, where \mathcal{V}_s is the set of nodes and \mathcal{E}_s is the set of edges (i, j) that signify the pairs of nodes $i, j \in \mathcal{V}_s$ between which the quadrotors can travel. A group of N quadrotors, indexed by the set \mathcal{N} , explores the environment using a random walk strategy: each quadrotor performs a random walk on the grid, moving from its current node i to an adjacent node j with transition probability p_{ij} at each discrete time k . We assume that each quadrotor is able to localize itself in this environment; i.e., that it knows which node it currently occupies. We also assume that quadrotors can communicate with one another only if they occupy the same node. We also assume that the quadrotors have perfect localization.

The number of targets estimated by each quadrotor is updated at every time step k . Let the i^{th} target detected by quadrotor a_j at time k be $m_{i,k}^{a_j} \in \mathbb{R}_+$ which is a tuple, composed of the *state* of the target, which is a time-varying property of the target like its location within the quadrotor's field of view (FoV), the pixels that it occupies in the quadrotor's camera image, and a unique identification label. Let $\mathcal{M}_k^{a_i} = \{m_{1,k}^{a_i}, \dots, m_{n_m,k}^{a_i}\}$ be the set of states of all targets detected by the quadrotor a_j at time k , where n_m is the maximum number of features that a quadrotor can detect simultaneously. The value of n_m is limited by the computational capabilities and the available memory on the robot. As the quadrotor explores the environment, the number of targets that it detects and their states vary, as new targets appear in the FoV of the quadrotor and existing targets disappear. An *observation set* obtained by a quadrotor at a particular time consists of both measurements that are associated with actual targets and measurements arising from clutter. The objective of multi-target tracking is to jointly estimate, at each time step, the number of targets and the targets' states from a series of noisy and cluttered observation sets. The concept of a *random finite set (RFS)* is useful for formulating this problem, since within the FoV of a quadrotor, the number of targets and their states are time-varying and not completely known. A random finite set, as defined in [16], is a set with a random number of elements which are themselves random. In other words, a RFS is a random variable whose possible values are unordered finite sets. A computationally tractable approach to set-based estimation is to utilize the first statistical moment of an RFS, known as the Probability Hypothesis Density (PHD) or its *intensity function*, for multi-target tracking. We propose to use the Gaussian Mixture formulation of the PHD filter (GM-PHD) for each quadrotor, as it is less computationally expensive than the particle filter implementation.

Figure 1 illustrates our multi-target tracking approach with two quadrotors and six stationary targets. The quadrotors explore the grid according to the random walk motion model defined in Section III, and they estimate the number of targets and their positions within their limited sensing FoV using the GM-PHD filter described in Section V.A. Sample trajectories are shown for each quadrotor as a sequence of arrows that indicate its direction of motion. At time step k , the first *renewal epoch*, the quadrotors meet at node m and exchange *rewards*, defined as each quadrotor's estimates of the number of targets that it has detected up until time k and their positions, as described in Section IV. The implementation of this strategy is described in pseudocode in Algorithm 1 and Algorithm 2. We extract only unique target states during simulation by using set union methods, as described in Algorithm 3.

III. Discrete-Time Discrete-Space (DTDS) Markov Chain Model of Robot Motion

Let $Y_k^{a_i} \in \mathcal{S}$ be the random variable that represents the location of quadrotor a_i at time k on the spatial grid. For each quadrotor a_i , the probability mass function $\pi_k \in \mathbb{R}^{1 \times S}$ of $Y_k^{a_i}$ evolves according to a discrete-time discrete-space (DTDS) Markov chain given by:

$$\pi_{k+1} = \mathbf{P}\pi_k, \quad (1)$$

where the *state transition matrix* $\mathbf{P} \in \mathbb{R}^{S \times S}$ has elements $p_{ij} \in [0, 1]$ at row i and column j . The time evolution of the probability mass function of $Y_k^{a_i}$ is expressed using the Markov property as follows:

$$Pr(Y_{k+1}^{a_i} = j_{k+1} | Y_k^{a_i} = j_k, \dots, Y_0^{a_i} = j_0) = Pr(Y_{k+1}^{a_i} = j_{k+1} | Y_k^{a_i} = j_k), \quad (2)$$

Algorithm 1: Control strategy for robot $a_i \in \mathcal{N}$

Step 0: Initialization $a_i, J_\gamma^{(a_i)}, \mu_\gamma^{(a_i)}, P_\gamma^{(a_i)}, Y_0^{(a_i)}, F_{k-1}, Q_{k-1}, H_k, R_k, \kappa_0^{(a_i)}(z), ps, pD, w_0^{(a_i)}, \mathcal{M}_0^{(\cdot)}$

Step 1: Random Walk

$$[Y_k^{(a_i)}] = \text{MarkovRandomWalk}(Y_{k-1}^{(a_i)});$$

Step 2: GM-PHD Filter

a Predicted State Components Apply steps 1 and 2 from Table 1 in [18]

$$J_{k-1}^{(a_i)} = J_\gamma^{(a_i)}; w_{k-1}^{(a_i)} = w_\gamma^{(a_i)}; \mu_{k-1}^{(a_i)} = \mu_\gamma^{(a_i)}$$

$$[w_{k|k-1}^{(a_i)}, \mu_{k|k-1}^{(a_i)}, P_{k|k-1}^{(a_i)}, J_{k|k-1}^{(a_i)}] = \text{predictGMPHD}(J_{k-1}^{(a_i)}, w_{k-1}^{(a_i)}, \mu_{k-1}^{(a_i)}, P_{k-1}^{(a_i)}, F_{k-1}, Q_{k-1}, ps);$$

b Updated State Components Apply steps 3 and 4 from Table 1 in [18]

$$[w_k, \mu_k, P_k, J_k] = \text{updateGMPHD}(H_k, \mu_{k|k-1}, R_k, P_{k|k-1}, pD, J_{k|k-1}, w_{k|k-1}, \kappa_k^{(a_i)}(z), Z_k^{(a_i)});$$

c Pruning and Merging Components Apply all steps from Table 2 in [18]

d Multi-target State Extraction Apply all steps from Table 3 in [18] with $thresh_{state} = 0.5$

$$[\hat{X}_k^{(a_i)}, \hat{w}_k^{(a_i)}, \hat{P}_k^{(a_i)}] = \text{extractMTStateGMPHD}(w_k^{(a_i)}, \mu_k^{(a_i)}, P_k^{(a_i)}, thresh_{state});$$

$$\mathcal{M}_k^{(a_i)} = \mathcal{M}_{k-1}^{(a_i)} \cup \hat{X}_k^{(a_i)};$$

where j_k is a specific node in the spatial grid that the quadrotor may occupy at time k . In other words, (2) states that the future location of the quadrotor depends only on its current location and is statistically independent of any previous locations. We assume that the DTDS Markov chain is time-homogeneous, which implies that $Pr(Y_{k+1}^{a_i} = j_{k+1} | Y_k^{a_i} = j_k)$ is same for all quadrotors at all time steps. Thus, the entries of \mathbf{P} can be defined as follows:

$$p_{ij} = Pr(Y_{k+1}^{a_i} = j_{k+1} | Y_k^{a_i} = j_k), \quad \forall j_k \in \mathcal{S}, k \in \mathbb{Z}_{\geq 0}, a_i \in \mathcal{N}. \quad (3)$$

Assuming that each quadrotor chooses its next position from a uniform random distribution, we can compute the entries of \mathbf{P} as follows:

$$p_{ij} = \begin{cases} \frac{1}{d_i+1}, & (i, j) \in \mathcal{E}_s, \\ 0, & \text{otherwise,} \end{cases} \quad (4)$$

where d_i is the degree of the node $i \in \mathcal{S}$. Since each entry $p_{ij} \geq 0$, we use the notation $\mathbf{P} \geq 0$. We see that $\mathbf{P}^m \geq 0$ for $m \geq 1$. Hence, \mathbf{P} is a *non-negative matrix*. Then, from Theorem 5 in [25], we can say that \mathbf{P} is a stochastic matrix. We define Equation 1 as the *spatial Markov chain*. From the construction of the spatial Markov chain, every quadrotor has a positive probability of moving from node $i \in \mathcal{S}$ to any node $j \in \mathcal{S}$ in a finite number of time steps. Thus, the Markov chain is said to be *irreducible*, and consequently, \mathbf{P} is an *irreducible matrix*. Now applying Lemma 8.4.4 in [26], we know that there exists a real unique positive left eigenvector of \mathbf{P} . Since \mathbf{P} is a stochastic matrix, we have that $\rho(\mathbf{P}) = 1$, where $\rho(\mathbf{P})$ denotes the spectral radius of \mathbf{P} . Thus, we can conclude that this real unique positive left eigenvector is the *stationary distribution* associated with the spatial Markov chain. Since we have shown that the Markov chain is irreducible and has a stationary distribution π that satisfies $\pi\mathbf{P} = \pi$, we can conclude from Theorem 21.12 in [27] that the Markov chain is *positive recurrent*. Thus, all states in the Markov chain are positive recurrent, which implies that each quadrotor will keep visiting every state on the finite spatial grid infinitely often. We will use this result to prove results on the associated renewal-reward process, which is discussed next.

IV. Renewal-Reward Process

We now define a random variable $\tau_j^{a_i} \in \mathbb{R}_{\geq 0}$ as the j^{th} interval between two successive times at which quadrotor a_i and any another quadrotor occupy the same node. This time interval is referred to as the *inter-arrival time*. A *renewal epoch* is a time instant at which two quadrotors meet at the same node. For each quadrotor a_i , we define the counting process $T^{a_i}(k) \in \mathbb{Z}_{\geq 0}$ as the number of times a_i has met any other quadrotor by time k . At each renewal epoch, quadrotor a_i updates its *reward*, defined as the number of all detected targets and their locations, with the number of targets and locations detected by the quadrotor(s) that occupies its current node and transmits this information to a_i . We use the definition of a *renewal process* given by Definition 7.1 in [28]. If the sequence of non-negative random variables $\{\tau_0^{a_i}, \tau_1^{a_i}, \dots\}$ is independent and identically distributed, then the counting process $T^{a_i}(k)$ is said to be a renewal process. We demonstrate that $T^{a_i}(k)$ is a renewal process at the end of this section.

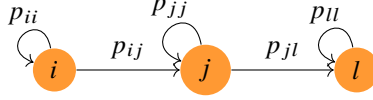


Fig. 2 An example graph $\mathcal{G}_s = (\mathcal{V}_s, \mathcal{E}_s)$ defined on the set of spatial nodes $\mathcal{V}_s = \{i, j, l\}$. The arrows signify directed edges between pairs of distinct nodes or self-edges. The edge set is $\mathcal{E}_s = \{(i, i), (j, j), (l, l), (i, j), (j, l)\}$.

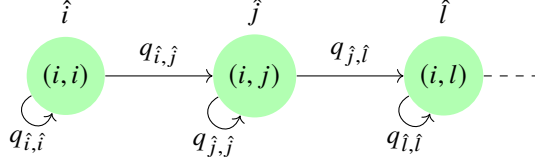


Fig. 3 A subset of the composite graph $\hat{\mathcal{G}} = (\hat{\mathcal{V}}, \hat{\mathcal{E}})$ for two agents that move on the graph \mathcal{G}_s shown in Figure 2.

For a renewal process having inter-arrival times $\tau_0^{a_i}, \tau_1^{a_i}, \dots$, we define $S_n^{a_i} = \sum_{j=1}^n \tau_j^{a_i}$ as the n^{th} renewal epoch, with $S_0^{a_i} = 0$ for all $a_i \in \mathcal{N}$. From the definition of a renewal process, we can infer that the number of renewal epochs by time k is greater than or equal to n if and only if the n^{th} renewal epoch occurs before or at time k ; that is,

$$T^{a_i}(k) \geq n \Leftrightarrow S_n^{a_i} \leq k. \quad (5)$$

Now consider that at each renewal epoch, quadrotor a_i receives a reward. The reward $R_n^{a_i}$ earned by quadrotor a_i when the n^{th} renewal occurs is defined as follows:

$$R_n^{a_i} = \mathcal{M}_k^{a_i} \bigcup_{a_j \neq a_i} \mathcal{M}_k^{a_j}, \quad Y_k^{a_i} = Y_k^{a_j} \text{ and } a_j \in \mathcal{N}. \quad (6)$$

Equation 5 and Equation 6 together define a *renewal-reward process*. Each quadrotor a_i calculates $\mathcal{M}_k^{a_i}$ by estimating the number of targets and their spatial distribution using a PHD filter. In Section V, we describe some fundamental theory on target detection and tracking using this type of filter.

Given the quadrotor motion model defined in Section III, we can model the dynamics of all the quadrotors' movements on the spatial grid by a composite Markov chain with states $\psi_k = (Y_k^{a_1}, Y_k^{a_2}, \dots, Y_k^{a_N}) \in \mathcal{H}$, where $\mathcal{H} = \mathcal{S}^N$. Note that $S = |\mathcal{S}|$ and $|\mathcal{H}| = S^N$. We now define another undirected graph $\hat{\mathcal{G}} = (\hat{\mathcal{V}}, \hat{\mathcal{E}})$ associated with this composite Markov chain. The vertex set $\hat{\mathcal{V}}$ is a set of all possible realizations $\hat{i} \in \mathcal{H}$ of ψ_k . Here $\hat{i}(a_l)$ represents the a_l^{th} entry of \hat{i} , which corresponds to the spatial node $i \in \mathcal{S}$ occupied by robot $a_l \in \mathcal{N}$ and $l \in \mathcal{I}$. We define the edge set $\hat{\mathcal{E}}$ of graph $\hat{\mathcal{G}}$ as follows: $(\hat{i}, \hat{j}) \in \hat{\mathcal{E}}$ if and only if $(\hat{i}(a_l), \hat{j}(a_l)) \in \mathcal{E}_s$ for all robots $a_l \in \mathcal{N}$. Let $\mathbf{Q} \in \mathbb{R}^{|\mathcal{H}| \times |\mathcal{H}|}$ be the state transition matrix associated with this composite Markov chain. An element of \mathbf{Q} , denoted by $q_{\hat{i}\hat{j}}$, is the probability that in the next time step, each robot a will move from spatial node $\hat{i}(a_l)$ to node $\hat{j}(a_l)$. These elements are computed from the transition probabilities defined by Equation (4) as follows:

$$q_{\hat{i}\hat{j}} = \prod_{a_l=1}^N p_{\hat{i}(a_l)\hat{j}(a_l)}, \quad \forall \hat{i}, \hat{j} \in \mathcal{H} \text{ \& } l \in \mathcal{I}. \quad (7)$$

As an illustration, consider a set of two robots, $\mathcal{N} = \{a_1, a_2\}$, that move on the graph \mathcal{G}_s shown in Figure 2. The robots can stay at their current node in the next time step or travel between nodes i and j and between nodes j and l , but they cannot travel between nodes i and l . Figure 3 shows a subset of the resulting composite graph $\hat{\mathcal{G}}$, which has the set of nodes $\hat{\mathcal{V}} = \{(i, i), (i, j), (i, l), (j, i), (j, j), (j, l), (l, i), (l, j), (l, l)\}$. Each node in $\hat{\mathcal{V}}$ is labeled by a single index \hat{i} , e.g., $\hat{i} = (i, j)$, with $\hat{i}(a_1) = i$ and $\hat{i}(a_2) = j$. Given the connectivity of the spatial grid defined by \mathcal{E}_s , we can for example identify $((i, j), (i, l))$ as an edge in $\hat{\mathcal{E}}$, but not $((i, j), (l, l))$. Since $N = 2$ and $S = 3$, we have that $|\mathcal{H}| = 3^2 = 9$. For each $\hat{i}, \hat{j} \in \hat{\mathcal{V}}$, we can compute the transition probabilities in $\mathbf{Q} \in \mathbb{R}^{9 \times 9}$ from Equation (7) as:

$$q_{\hat{i}\hat{j}} = Pr(\psi_{k+1} = \hat{j} \mid \psi_k = \hat{i}) = p_{\hat{i}(a_1)\hat{j}(a_1)} p_{\hat{i}(a_2)\hat{j}(a_2)}, \quad k \in \mathbb{Z}_+. \quad (8)$$

We now prove that $T^{a_i}(k)$ is a renewal process.

Theorem IV.1. $T^{a_i}(k)$ is a renewal process on the composite Markov chain ψ_k .

Proof. Suppose that an initial time instant k_0 , the locations of all N robots on the spatial grid are represented by the node $\hat{i} \in \hat{\mathcal{V}}$. Consider another set of robot locations at time $k_0 + k$, where $k > 0$, represented by the node $\hat{j} \in \hat{\mathcal{V}}$. The transition of the robots from configuration \hat{i} to configuration \hat{j} in k time steps corresponds to a random walk of length k on the composite Markov chain ψ_k from node \hat{i} to node \hat{j} . It also corresponds to a random walk by each robot a_i on the spatial grid from node $\hat{i}(a_i)$ to node $\hat{j}(a_i)$ in k time steps. By construction, the graph \mathcal{G}_s is strongly connected and each of its nodes has a self-edge. Therefore, there exists a discrete time $n > 0$ such that, for each robot $a_i \in \mathcal{N}$, there exists a random walk on the spatial grid from node $\hat{i}(a_i)$ to node $\hat{j}(a_i)$ in n time steps. Consequently, there always exists a random walk of length n on the composite Markov chain ψ_k from node \hat{i} to node \hat{j} . Therefore, ψ_k is an irreducible Markov chain. All states of an irreducible Markov chain belong to a single communication class. In this case, all states are *positive recurrent*. As a result, ψ_k is *positive recurrent*. Thus, each state in ψ_k is visited infinitely often from all other states in ψ_k . A state with this property is said to *regenerate* (or *renew*) infinitely often. We can then conclude from Proposition 67 in [29] that $T^{a_i}(k)$ is a regenerative process on ψ_k . Since every regenerative process is a renewal process, $T^{a_i}(k)$ is a renewal process. \square

Algorithm 2: Renewal-reward computation for robots $(a_i, a_j) \in \mathcal{N}$

```

Given:  $\mathcal{M}_k^{(a_i)}, \mathcal{M}_k^{(a_j)}, Y_k^{(a_i)}, Y_k^{(a_j)}$ 
for  $k \in 1 : t_{final}$  do
  for  $n_1 \in 1 : |\mathcal{N}|$  do
     $l = 1; n = 1;$ 
    for  $n_2 \in n_1 + 1 : |\mathcal{N}|$  do
      if  $Y_k^{(n_1)} = Y_k^{(n_2)}$  then
         $R_n^l = \mathcal{M}_k^{(n_1)} \cup \mathcal{M}_k^{(n_2)};$ 
         $l = l + 1; n = n + 1;$ 
      end
    end
  end
end

```

Algorithm 3: Exchange of set of estimated states between robots $(a_i, a_j) \in \mathcal{N}$

```

Given:  $X_{k-1}^{(a_i, a_j)}, \hat{X}_k^{(a_i)}, \hat{X}_k^{(a_j)}$ 
for  $l_1 \in 1 : size(|\hat{X}_k^{(a_i)}|, 2)$  do
  for  $l_2 \in 1 : size(|\hat{X}_k^{(a_j)}|, 2)$  do
     $X_{temp} = \hat{X}_{k, l_1}^{(a_i)} \cup \hat{X}_{k, l_2}^{(a_j)};$ 
    if  $X_{temp} \not\subseteq X_{k-1}^{(a_i, a_j)}$  then
       $X_k^{(a_i, a_j)} = X_{k-1}^{(a_i, a_j)} \cup X_{temp};$ 
    end
    else
       $X_k^{(a_i, a_j)} = X_{k-1}^{(a_i, a_j)};$ 
    end
  end
end
 $\mathcal{M}_k^{(a_i, a_j)} = X_k^{(a_i, a_j)};$ 
end

```

V. Random Finite Sets Based Probability Hypothesis Density Filter

Let $M_k^{a_i} \leq n_m$ be the number of targets identified by quadrotor a_i at time step k . Suppose that at time $k-1$, the target states are $x_{k-1,1}^{a_i}, x_{k-1,2}^{a_i}, \dots, x_{k-1,M_{k-1}^{a_i}}^{a_i} \in \mathcal{X}$, where \mathcal{X} is the set of target states. At the next time step, some of these targets might disappear from the quadrotor's field of view (FoV), and new targets may appear. This results in $M_k^{a_i}$ new states $x_{k,1}^{a_i}, x_{k,2}^{a_i}, \dots, x_{k,M_k^{a_i}}^{a_i}$. Note that the order in which the states are represented has no significance in the RFS multi-target tracking formulation. The quadrotor a_i makes $N_k^{a_i}$ measurements $z_{k,1}^{a_i}, \dots, z_{k,N_k^{a_i}}^{a_i} \in \mathcal{Z}$ at time k , where \mathcal{Z} is the set of measurements. The order in which the measurements are made is not significant. The states of the targets identified by quadrotor a_i at time k (i.e., the multi-target state) and the measurements obtained by the quadrotor at time k can both be represented as finite sets:

$$X_k^{a_i} = \{x_{k,1}^{a_i}, \dots, x_{k,M_k^{a_i}}^{a_i}\} \in \mathcal{F}(\mathcal{X}), \quad (9)$$

$$Z_k^{a_i} = \{z_{k,1}^{a_i}, \dots, z_{k,N_k^{a_i}}^{a_i}\} \in \mathcal{F}(\mathcal{Z}), \quad (10)$$

where $\mathcal{F}(\mathcal{X})$ is the multi-target state space and $\mathcal{F}(\mathcal{Z})$ is the measurement space. For a quadrotor a_i , given multi-target state $X_{k-1}^{a_i}$ at time $k-1$, each $x_{k-1}^{a_i} \in X_{k-1}^{a_i}$ either continues to exist (survives) at time k with probability $p_{S,k}^{a_i}(x_{k-1}^{a_i})$ or disappears (dies) at time k with probability $1 - p_{S,k}^{a_i}(x_{k-1}^{a_i})$. The conditional probability density at time k of a transition from state $x_{k-1}^{a_i}$ to state $x_k^{a_i}$ is given by $f_{k|k-1}^{a_i}(\cdot|\cdot)$.

We now define the RFS model for the time evolution of the multi-target state, which incorporates motion of the targets relative to the quadrotor, appearance (birth) of targets, and disappearance (death) of targets:

$$X_k^{a_i} = \left[\bigcup_{\xi \in X_{k-1}^{a_i}} \mathbf{S}_{k|k-1}^{a_i}(\xi) \right] \cup \left[\bigcup_{\xi \in X_{k-1}^{a_i}} \mathbf{B}_{k|k-1}^{a_i}(\xi) \right] \cup \mathbf{\Gamma}_k^{a_i} \quad (11)$$

- $\mathbf{S}_{k|k-1}^{a_i}(\xi)$: RFS of targets with previous state ξ at time $k-1$ that survive at time k
- $\mathbf{B}_{k|k-1}^{a_i}(\xi)$: RFS of targets spawned at time k from targets with previous state ξ at time $k-1$
- $\mathbf{\Gamma}_k^{a_i}$: RFS of targets that are spontaneously born at time k

At each time step, a quadrotor a_i detects a target with state $x_k^{a_i} \in X_k^{a_i}$ with probability $p_{D,k}^{a_i}(\cdot)$, or misses it with probability $1 - p_{D,k}^{a_i}(\cdot)$. The conditional probability of obtaining a measurement $z_k^{a_i} \in Z_k^{a_i}$ from $x_k^{a_i}$ is characterized by the multi-target likelihood function, $g_k^{a_i}(\cdot|\cdot)$. We can now define the RFS model for the time evolution of the multi-target measurement, which incorporates measurements of actual targets along with clutter:

$$Z_k^{a_i} = \mathbf{K}_k^{a_i} \cup \left[\bigcup_{x \in X_k^{a_i}} \mathbf{\Theta}_k^{a_i}(x) \right] \quad (12)$$

- $\mathbf{K}_k^{a_i}$: RFS of measurements arising from clutter at time k
- $\mathbf{\Theta}_k^{a_i}(x)$: RFS of measurements of the multi-target state $X_k^{a_i}$ at time k

The multi-target Bayes filter propagates the multi-target posterior density $p_k^{a_i}(\cdot | Z_{1:k}^{a_i})$ in time via recursion as:

$$p_{k|k-1}^{a_i}(X_k^{a_i} | Z_{1:k-1}^{a_i}) = \int_{X^{a_i} \in \mathcal{F}(\mathcal{X})} f_{k|k-1}^{a_i}(X_k^{a_i} | X^{a_i}) p_{k-1}^{a_i}(X^{a_i} | Z_{1:k-1}^{a_i}) \mu_S(dX^{a_i}) \quad (13)$$

$$p_k^{a_i}(X_k^{a_i} | Z_{1:k}^{a_i}) = \frac{g_k^{a_i}(Z_k^{a_i} | X_k^{a_i}) p_{k|k-1}^{a_i}(X_k^{a_i} | Z_{1:k-1}^{a_i})}{\int_{X^{a_i} \in \mathcal{F}(\mathcal{X})} g_k^{a_i}(Z_k^{a_i} | X^{a_i}) p_{k|k-1}^{a_i}(X^{a_i} | Z_{1:k-1}^{a_i}) \mu_S(dX^{a_i})} \quad (14)$$

where μ_S is a suitable reference measure on $\mathcal{F}(\mathcal{X})$ of target states $X^{a_i} \in \mathcal{F}(\mathcal{X})$, $g_k^{a_i}(\cdot|\cdot)$ represents the multi-target likelihood function, and $f_{k|k-1}^{a_i}(\cdot|\cdot)$ represents the multi-target transition density. For further details, see [17, 18].

We will approximate the integrals above using the framework of the probability hypothesis density (PHD) filter, with the assumptions that: (1) each target evolves and generates observations independently of the others; (2) clutter is Poisson distributed and independent of target-originated measurements; (3) the multi-target RFS is Poisson distributed. For a RFS $X^{a_i} \in \mathcal{X}$ with probability distribution $p^{a_i}(\cdot)$, there is a non-negative function v on \mathcal{X} , defined as the *intensity function*, such that for each region $\mathcal{S} \subset \mathcal{X}$,

$$\int |X^{a_i} \cap \mathcal{S}| p^{a_i}(dX) = \int_{\mathcal{S}} v(x) dx. \quad (15)$$

Then we can model the posterior intensity and its recursion as follows:

$$v_{k|k-1}^{a_i}(x) = \int p_{\mathbf{S},k}^{a_i}(\xi) f_{k|k-1}^{a_i}(x|\xi) v_{k-1}^{a_i}(\xi) d\xi + \int \beta_{k|k-1}^{a_i}(x|\xi) v_{k-1}^{a_i}(\xi) d\xi + \gamma_k^{a_i}(x), \quad (16)$$

$$v_k^{a_i}(x) = [1 - p_{\mathbf{D},k}^{a_i}(x)] v_{k|k-1}^{a_i}(x) + \sum_{z \in \mathcal{Z}_k^{a_i}} \frac{p_{\mathbf{D},k}^{a_i}(x) g_k^{a_i}(z|x) v_{k|k-1}^{a_i}(x)}{\kappa_k^{a_i}(z) + \int p_{\mathbf{D},k}^{a_i}(\xi) g_k^{a_i}(z|\xi) v_{k|k-1}^{a_i}(\xi)}. \quad (17)$$

In these equations, $v_k^{a_i}$ and $v_{k|k-1}^{a_i}$ denote the intensities associated with, respectively, the multi-target posterior density $p_k^{a_i}(\cdot|\cdot)$ and the multi-target predicted density $p_{k|k-1}^{a_i}(\cdot|\cdot)$ that are defined by the recursion in Equation 13 and Equation 14. The function $\gamma_k^{a_i}(\cdot)$ is the intensity of the RFS $\mathbf{\Gamma}_k^{a_i}$, $\beta_{k|k-1}^{a_i}(\cdot|\xi)$ is the intensity of the RFS $\mathbf{B}_{k|k-1}(\xi)$, and $\kappa_k^{a_i}(\cdot)$ is the intensity of the RFS $\mathbf{K}_k^{a_i}$. The quadrotor a_i can estimate the number of targets as

$$\hat{N} = \int v(x) dx. \quad (18)$$

The estimate \hat{N} is used to update the number of elements of $\mathcal{M}_k^{a_i}$, and the intensity $v_k^{a_i}(x)$ computed from Equation 17 is used to update the states of the \hat{N} targets. Then each element of $\mathcal{M}_k^{a_i}$ is represented as the following tuple:

$$m_{k,l}^{a_i} = \langle l, v_k^{a_i}(x) \rangle, \quad (19)$$

where l is a label for the tracked target, such as one of its properties, e.g. its color, shape, size or its position in the environment.

A. Gaussian Mixture PHD Filter

The PHD filter as described in (16) and (17) does not admit a closed-form solution in general, and the numerical integration suffers from the curse of dimensionality. Thus, for implementation purposes, we consider a sub-optimal solution of the PHD filter that models approximates it as a mixture of Gaussians, as described in [18]. The Gaussian Mixture PHD (GM-PHD) filter provides a closed-form solution to the PHD filter under the following assumptions:

- A.1** Each target generates observations independently of the others.
- A.2** The clutter process is Poisson distributed and is independent of target-generated measurements.
- A.3** Each target's state evolves according to a linear model with Gaussian process noise, and each quadrotor's sensor has a linear measurement model with Gaussian sensor noise, i.e.

$$f_{k|k-1}^{a_i}(x|\xi) = \mathbb{N}(x; F_{k-1}, Q_{k-1}), \quad (20)$$

$$g_k^{a_i}(z|\xi) = \mathbb{N}(z; H_k x, R_k), \quad (21)$$

where the notation $\mathbb{N}(\cdot; \mu, \sigma)$ denotes a Gaussian density with mean μ and covariance σ , F_{k-1} is the state transition matrix, Q_{k-1} is the process noise covariance, H_k is the observation or measurement matrix, and R_k is the sensor noise covariance.

- A.4** The detection probability is state-dependent and is modeled as

$$p_{\mathbf{D},k}^{a_i}(x) = \begin{cases} p_{\mathbf{D}} & \|q_k^{a_i} - x\| \in \mathcal{B}_r(q_k^{a_i}), \\ 0 & \text{otherwise,} \end{cases} \quad (22)$$

where $q_k^{a_i}$ denotes the grid coordinates of robot a_i at time k and $\mathcal{B}_r(q_k^{a_i})$ represents the FoV of the sensor on robot a_i , which we model as a disc of radius r centered at the robot location $q_k^{a_i}$. The survival probability is assumed to be constant:

$$p_{\mathbf{S},k}^{a_i}(x) = p_{\mathbf{S},k}. \quad (23)$$

A.5 The birth and spawning intensities are modeled as Gaussian mixtures of the form

$$\gamma_k^{a_i}(x) = \sum_{i=1}^{J_{\gamma,k}} w_{\gamma,k}^{(i)} \mathbb{N}(x; \mu_{\gamma,k}^{(i)}, P_{\gamma,k}^{(i)}), \quad (24)$$

$$\beta_{k|k-1}^{a_i}(x|\xi) = \sum_{j=1}^{J_{\beta,k}} w_{\beta,k}^{(j)} \mathbb{N}(x; F_{\beta,k-1}^{(j)} \xi + d_{\beta,k-1}^{(j)}, Q_{\beta,k-1}^{(j)}), \quad (25)$$

where $J_{\gamma,k}$, $w_{\gamma,k}^{(i)}$, $\mu_{\gamma,k}^{(i)}$, and $P_{\gamma,k}^{(i)}$ are known parameters of the birth intensity, and $J_{\beta,k}$, $w_{\beta,k}^{(j)}$, $F_{\beta,k-1}^{(j)}$, $d_{\beta,k-1}^{(j)}$, $Q_{\beta,k-1}^{(j)}$, and $P_{\beta,k-1}^{(j)}$ are known parameters of the spawn intensity of a target with state ξ at time $k-1$. For more details on the parameters, please refer to [18].

Using the above assumptions, we can rewrite Equation 16 and Equation 17 as follows. The intensity associated with the multi-target predicted density can be approximated as a Gaussian mixture:

$$v_{k|k-1}^{a_i}(x) = v_{\mathbf{S},k|k-1}^{a_i}(x) + v_{\beta,k|k-1}^{a_i}(x) + \gamma_k^{a_i}(x), \quad (26)$$

where

$$v_{\mathbf{S},k|k-1}^{a_i}(x) = p_{\mathbf{S},k} \sum_{i=1}^{J_{k-1}} w_{k-1}^{(i)} \mathbb{N}(x; \mu_{\mathbf{S},k|k-1}^{(i)}, P_{\mathbf{S},k|k-1}^{(i)}), \quad (27)$$

$$\mu_{\mathbf{S},k|k-1}^{(i)} = F_{k-1} \mu_{k-1}^{(i)}, \quad (28)$$

$$P_{\mathbf{S},k|k-1}^{(i)} = Q_{k-1} + F_{k-1} P_{k-1}^{(i)} F_{k-1}^T, \quad (29)$$

$$v_{\beta,k|k-1}^{a_i}(x) = \sum_{i=1}^{J_{k-1}} \sum_{l=1}^{J_{\beta,k}} w_{k-1}^{(i)} w_{\beta,k}^{(l)} \mathbb{N}(x; \mu_{\beta,k|k-1}^{(i,l)}, P_{\beta,k|k-1}^{(i,l)}), \quad (30)$$

$$\mu_{\beta,k|k-1}^{(i,l)} = F_{\beta,k-1} \mu_{k-1}^{(i)} + d_{\beta,k-1}^{(l)}, \quad (31)$$

$$P_{\beta,k|k-1}^{(i,l)} = Q_{\beta,k-1}^{(l)} + F_{\beta,k-1} P_{\beta,k-1}^{(i)} (F_{\beta,k-1}^{(l)})^T, \quad (32)$$

in which J_{k-1} , $w_{k-1}^{(i)}$, $\mu_{k-1}^{(i)}$, and $P_{k-1}^{(i)}$ are known parameters of the intensity function at time $k-1$ [18].

Then the intensity associated with the multi-target posterior density can be approximated as a Gaussian mixture:

$$v_k^{a_i}(x) = [1 - p_{\mathbf{D},k}^{a_i}(x)] v_{k|k-1}^{a_i}(x) + \sum_{z \in Z_k^{a_i}} v_{\mathbf{D},k}^{a_i}(x; z), \quad (33)$$

where

$$v_{\mathbf{D},k}^{a_i}(x; z) = \sum_{j=1}^{J_{k|k-1}} w_k^{(j)}(z) \mathbb{N}(x; \mu_{k|k}^{(j)}(z), P_{k|k}^{(j)}), \quad (34)$$

$$w_k^{(j)}(z) = \frac{p_{\mathbf{D},k}^{a_i}(x) w_{k|k-1}^{(j)} \mathbb{N}(z; H_k \mu_{k|k-1}, R_k + H_k P_k H_k^T)}{\kappa_k^{a_i}(z) + p_{\mathbf{D},k}^{a_i}(x) \sum_{l=1}^{J_{k|k-1}} w_{k|k-1}^{(l)} \mathbb{N}(z; H_k \mu_{k|k-1}, R_k + H_k P_k H_k^T)}, \quad (35)$$

$$\mu_{k|k}^{(j)}(z) = \mu_{k|k-1}^{(j)}(z) + K_k^{(j)}(z - H_k \mu_{k|k-1}^{(j)}(z)), \quad (36)$$

$$P_{k|k}^{(j)} = [I - K_k^{(j)} H_k] P_{k|k-1}^{(j)}, \quad (37)$$

$$K_k^{(j)} = P_{k|k-1}^{(j)} H_k^T [H_k P_{k|k-1}^{(j)} H_k^T + R_k]^{-1}. \quad (38)$$

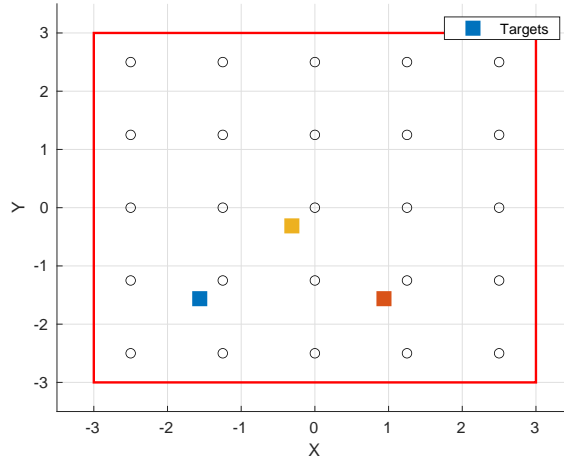


Fig. 4 A $5\text{m} \times 5\text{m}$ square environment, with hollow circles denoting the grid nodes and squares denoting the targets. The red border denotes the boundary of the area that is explored by 3 robots.

VI. Simulation Results

In this section, we validate our approach with simulations in MATLAB. First, we model a scenario with a bounded environment with dimensions $5\text{m} \times 5\text{m}$ that contains 3 stationary targets which must be located by 3 robots, as shown in Figure 4. The state of each target is defined as its $x - y$ position coordinates, $x = [p_x, p_y]^T$. A robot's sensor measurement of a target's state is modeled according to Equation (21). Each robot has a circular FoV of radius $r_{FOV} = 0.6\text{m}$, centered at the robot's position on the spatial grid. We assume that each robot is able to accurately localize itself on the grid, and that there are no obstacles present in the environment.

Since each agent has a limited FoV, We assume that the targets that are detected at time step k survive in the next time step with probability $p_{S,k} = 0.1$ for all robots. Since the targets are stationary, $F_{k-1} = \mathbf{I}_2$, the 2×2 identity matrix. We also set $Q_{k-1} = 0.2\mathbf{I}_2$. As the robots explore the environment, new targets might appear in their FoV. We account for this by allowing 4 new targets to be birthed at each time step, depending upon the robot's position on the grid, with weights $w_{\gamma,k} = (w_{\gamma,k}^{(i)})_{i=1}^4 = [0.1, 0.1, 0.1, 0.1]^T$. Thus, the birth intensity at each time step from Equation (24) is modeled as

$$\gamma_k^{a_i}(x) = 0.1\mathbb{N}(x; \mu_{\gamma,k}^{(1)}, P_{\gamma,k}^{(1)}) + 0.1\mathbb{N}(x; \mu_{\gamma,k}^{(2)}, P_{\gamma,k}^{(2)}) + 0.1\mathbb{N}(x; \mu_{\gamma,k}^{(3)}, P_{\gamma,k}^{(3)}) + 0.1\mathbb{N}(x; \mu_{\gamma,k}^{(4)}, P_{\gamma,k}^{(4)}), \quad (39)$$

where $P_{\gamma}^{(l)} = 0.5\mathbf{I}_2$ and

$$\mu_{\gamma}^{(l)} = \begin{bmatrix} p_{x,k}^{a_i} + r_{birth} \cos(\theta_l) \\ p_{y,k}^{a_i} + r_{birth} \sin(\theta_l) \end{bmatrix}, \quad (40)$$

in which $q_k^{a_i} = [p_{x,k}^{a_i}, p_{y,k}^{a_i}]$ denotes the $x - y$ coordinates of robot a_i at time step k , corresponding to its current node $Y_k^{a_i}$; $r_{birth} = 0.8r_{FOV}$, so that the targets are birthed only near the boundary of FOV; and $\theta_l = [\pi/4, 3\pi/4, 5\pi/4, 7\pi/4]^T$ rad, the angles at which targets are likely to appear. We assume that there are no spawned targets. Each target is detected with a probability of $p_{\mathbf{D}} = 0.8$, and a quadrotor's observation of a target follows the measurement model (21) with $H_k = \mathbf{I}_2$ and $R_k = 0.25\mathbf{I}_2$. The observations are immersed in clutter that can be modeled as a Poisson RFS $\mathbf{K}_k^{(\cdot)}$ with intensity $\kappa_k^{(\cdot)}(z) = \lambda_C A_s \mathbb{U}(z)$, where $\lambda_C = 3.98 \times 10^{-3}$ is the clutter intensity; A_s is the area of the sensor's circular FoV, which is approximately 1m^2 ; and $\mathbb{U}(z)$ is the uniform density over A_s .

We assume that all robots start at random positions on the grid and have no knowledge of the number of targets or their states (positions). The robots explore the environment according to the random walk model (1). As the robots detect the targets, they recursively update their estimates of the number of targets and their positions using the GM-PHD framework described in Section V.A. We set $T = 1 \times 10^{-3}$ as the pruning threshold and $U = 4$ as the merging distance threshold (see Table II in [18] for details on these parameters). Figure 5a plots the inter-arrival times over time during 300 s of the simulation. Each inter-arrival time $\tau_j^{am^{an}}$ ends at a renewal epoch, i.e. a time when any two robots a_m

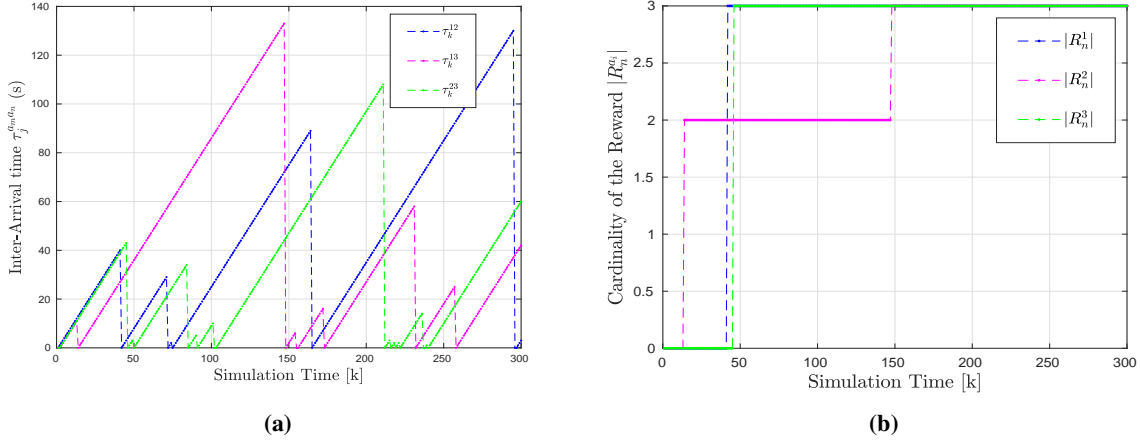


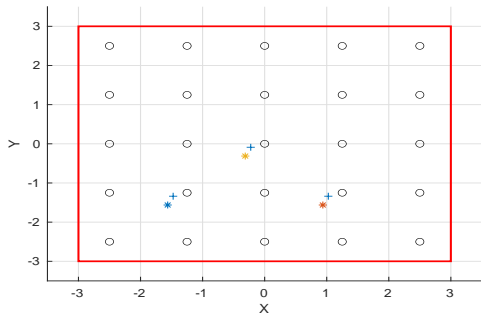
Fig. 5 (a) Inter-arrival times during a simulation of 3 robots exploring the environment in Figure 4. Renewal epochs, i.e. times when two robots meet at a node, are the times at the peaks of the graphs. Each renewal epoch marks the initialization of a new inter-arrival time. (b) Cardinality of the reward accumulated by each of the robots at each time step.

and a_n meet at a node, which can be identified in the figure as the time at the corresponding peak of the graph. At this time, the next inter-arrival time $\tau_{j+1}^{a_m a_n}$ is initialized to zero. Figure 5b plots the time evolution of the cardinality of the reward (6) earned by each robot, which is the estimated number of targets. The average inter-arrival time over this simulation run was calculated to be $\mathbb{E}[\tau_k^{(\cdot)}] \sim 68$ s, and the time required for the cardinality of all robots' rewards to equal the actual number of targets, $n = 3$, was $t_{reward} \sim 150$ s. Thus, for a scenario with both a robot density (number of robots per m^2) and a target density (number of targets per m^2) of $3/25 = 0.12$ m^{-2} , there must be about $\frac{t_{reward}}{\mathbb{E}[\tau_j^{(\cdot)}]} \approx 2.2$ renewals, i.e. at least 2 renewals, for all robots to achieve the same reward cardinality (estimated number of targets). Figure 6a, Figure 7a, and Figure 8a show the true positions of the targets and their estimated positions by each robot at the end of the simulation time. Figure 6b, Figure 7b, and Figure 8b show the corresponding PHD intensity for each robot as a Gaussian mixture model with $n = 3$ components (the number of targets), computed from Equation (33). We obtain the number of targets estimated by each robot a_i as

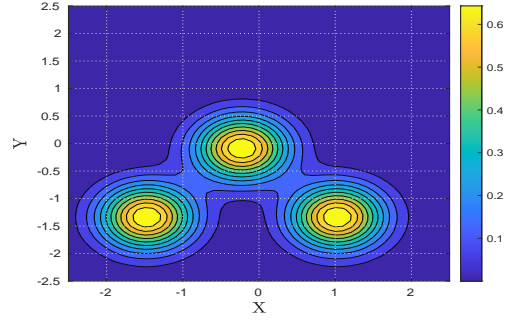
$$\hat{N}^{a_i} = \left[\sum_{k=1}^n w_k^{(l), a_i} \right], \quad (41)$$

where the weights $w_k^{(\cdot), a_i}$ for robots $a_i = 1, 2, 3$ are given by the peak intensities in Figure 6b, Figure 7b, and Figure 8b, respectively. The estimated positions of the targets are obtained from positions of these peak intensities.

We also evaluated our approach through Monte Carlo simulations of three scenarios, with 100 simulation runs for each scenario. In all scenarios, 20 robots explored a grid according to the random walk model (1) in order to track a set of stationary targets. The robots were initialized at random positions on the grid, and the positions of the targets were kept the same over all 100 runs for each scenario. In Scenario 1, simulated for 1000 s, the grid has dimensions $15m \times 15m$ and there are 10 targets; in Scenario 2, simulated for 2000 s, the grid has dimensions $20m \times 20m$ and there are 15 targets; and in Scenario 3, simulated for 3000 s, the grid has dimensions $30m \times 30m$ and there are 20 targets. The mean inter-arrival time and mean reward percentage for each scenario, averaged over all 100 runs, are given in Table 1. The mean reward percentage is computed from the ratio of the mean number of targets detected by the robots until the mean inter-arrival time to the actual number of targets in the scenario. Table 1 shows that the mean inter-arrival time increases as the density of robots in the environment decreases, which is due to the lower rate of robots encounters with one another in larger environments, on average. The table also shows that as the density of targets in the environment decreases, the percentage of targets identified before the mean inter-arrival time increases, on average. This indicates that in the scenarios simulated, the longer inter-arrival times for larger environments tend to enable identification of a higher number of targets, despite the lower target density.

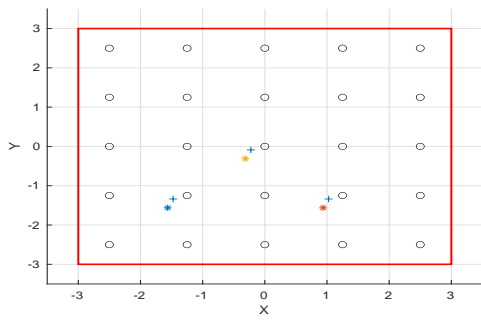


(a)

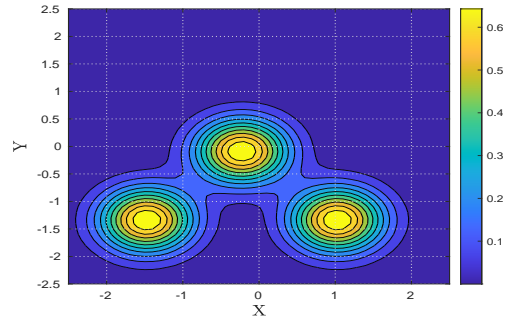


(b)

Fig. 6 Multi-target tracking by robot 1. (a) Estimated (*) and true (+) target positions. (b) GM-PHD intensities computed from Equation (33).

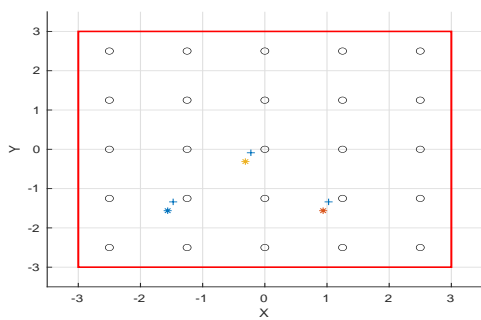


(a)

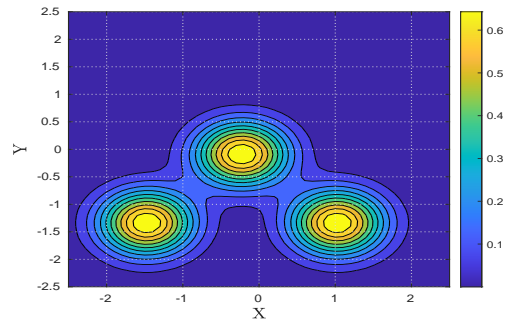


(b)

Fig. 7 Multi-target tracking by robot 2. (a) Estimated (*) and true (+) target positions. (b) GM-PHD intensities computed from Equation (33).



(a)



(b)

Fig. 8 Multi-target tracking by robot 3. (a) Estimated (*) and true (+) target positions. (b) GM-PHD intensities computed from Equation (33).

Scenarios	1	2	3
Mean inter-arrival time (s)	20	190	430
Mean reward (%)	10	33	65

Table 1 Mean inter-arrival time and mean reward percentage over 100 simulation runs each for 3 scenarios.

VII. Conclusion and Future Work

In this paper, we demonstrated theoretically that a group of robots equipped with limited sensing and communication capabilities, moving according to a DTDS Markov chain model on a spatial grid, is able to detect and track the number and states of multiple stationary targets in the environment using the Gaussian Mixture formulation of the PHD filter from the RFS framework. We verified our results with numerical simulations in MATLAB. In the future, we plan to implement this strategy on quadrotors equipped with RGBD cameras and 5G WiFi dongles for exchanging data between the robots.

VIII. Acknowledgments

This work was supported by the Arizona State University Global Security Initiative. The authors utilized HPC resources provided by Research Computing at Arizona State University to generate results reported in this paper.

References

- [1] Buhmann, J., Burgard, W., Cremers, A. B., Fox, D., Hofmann, T., Schneider, F. E., Strikos, J., and Thrun, S., “The mobile robot Rhino,” *AI Magazine*, Vol. 16, No. 2, 1995, p. 31.
- [2] Achtelik, M., Bachrach, A., He, R., Prentice, S., and Roy, N., “Autonomous navigation and exploration of a quadrotor helicopter in GPS-denied indoor environments,” *First Symposium on Indoor Flight*, Citeseer, 2009.
- [3] Michael, N., Shen, S., Mohta, K., Kumar, V., Nagatani, K., Okada, Y., Kiribayashi, S., Otake, K., Yoshida, K., Ohno, K., et al., “Collaborative mapping of an earthquake damaged building via ground and aerial robots,” *Field and Service Robotics*, Springer, 2014, pp. 33–47.
- [4] Burgard, W., Moors, M., Stachniss, C., and Schneider, F. E., “Coordinated multi-robot exploration,” *IEEE Transactions on Robotics*, Vol. 21, No. 3, 2005, pp. 376–386.
- [5] Grocholsky, B., Keller, J., Kumar, V., and Pappas, G., “Cooperative air and ground surveillance,” *IEEE Robotics & Automation Magazine*, Vol. 13, No. 3, 2006, pp. 16–26.
- [6] Simmons, R., Apfelbaum, D., Burgard, W., Fox, D., Moors, M., Thrun, S., and Younes, H., “Coordination for multi-robot exploration and mapping,” *AAAI/IAAI*, 2000, pp. 852–858.
- [7] Howard, A., Parker, L. E., and Sukhatme, G. S., “Experiments with a large heterogeneous mobile robot team: Exploration, mapping, deployment and detection,” *The International Journal of Robotics Research*, Vol. 25, No. 5-6, 2006, pp. 431–447.
- [8] Husain, A., Jones, H., Kannan, B., Wong, U., Pimentel, T., Tang, S., Daftry, S., Huber, S., and Whittaker, W. L., “Mapping planetary caves with an autonomous, heterogeneous robot team,” *2013 IEEE Aerospace Conference*, IEEE, 2013, pp. 1–13.
- [9] Daley, D. J., and Vere-Jones, D., *An introduction to the theory of point processes: volume II: general theory and structure*, Springer Science & Business Media, 2007.
- [10] Jensfelt, P., and Kristensen, S., “Active global localization for a mobile robot using multiple hypothesis tracking,” *IEEE Transactions on Robotics and Automation*, Vol. 17, No. 5, 2001, pp. 748–760.
- [11] Reid, D., “An algorithm for tracking multiple targets,” *IEEE Transactions on Automatic Control*, Vol. 24, No. 6, 1979, pp. 843–854.
- [12] Bar-Shalom, Y., and Fortmann, T. E., *Tracking and data association*, Mathematics in Science and Engineering, Vol. 179, Elsevier Science, 1988.

- [13] Schulz, D., Burgard, W., Fox, D., and Cremers, A. B., "Tracking multiple moving objects with a mobile robot," *Proceedings of the 2001 IEEE Computer Society Conference on Computer Vision and Pattern Recognition. CVPR 2001*, Vol. 1, IEEE, 2001.
- [14] Mahler, R., Hall, D., and Llinas, J., "Random set theory for target tracking and identification," *Data Fusion Hand Book*, CRC Press Boca Raton, 2001, p. 14.
- [15] Mahler, R. P., "Multitarget Bayes filtering via first-order multitarget moments," *IEEE Transactions on Aerospace and Electronic systems*, Vol. 39, No. 4, 2003, pp. 1152–1178.
- [16] Mahler, R. P., *Statistical multisource-multitarget information fusion*, Vol. 685, Artech House Norwood, MA, 2007.
- [17] Clark, D. E., Panta, K., and Vo, B.-N., "The GM-PHD filter multiple target tracker," *2006 9th International Conference on Information Fusion*, IEEE, 2006, pp. 1–8.
- [18] Vo, B.-N., and Ma, W.-K., "The Gaussian mixture probability hypothesis density filter," *IEEE Transactions on Signal Processing*, Vol. 54, No. 11, 2006, pp. 4091–4104.
- [19] Sung, Y., and Tokekar, P., "Algorithm for searching and tracking an unknown and varying number of mobile targets using a limited fov sensor," *2017 IEEE International Conference on Robotics and Automation (ICRA)*, IEEE, 2017, pp. 6246–6252.
- [20] Kamath, S., Meisner, E., and Isler, V., "Triangulation based multi target tracking with mobile sensor networks," *Proceedings 2007 IEEE International Conference on Robotics and Automation*, IEEE, 2007, pp. 3283–3288.
- [21] Dames, P., and Kumar, V., "Cooperative multi-target localization with noisy sensors," *2013 IEEE International Conference on Robotics and Automation (ICRA)*, IEEE, 2013, pp. 1877–1883.
- [22] Dames, P. M., "Distributed multi-target search and tracking using the PHD filter," *Autonomous Robots*, 2019, pp. 1–17.
- [23] Hung, P. D., Vinh, T. Q., and Ngo, T. D., "A scalable, decentralised large-scale network of mobile robots for multi-target tracking," *Intelligent Autonomous Systems 13*, Springer, 2016, pp. 621–637.
- [24] Shirsat, A., Elamvazhuthi, K., and Berman, S., "Multi-Robot Target Search using Probabilistic Consensus on Discrete Markov Chains," , 2020. Accepted to the *IEEE International Symposium on Safety, Security, and Rescue Robotics (SSRR)*. Preprint available at: <https://www.researchgate.net/publication/344324268>.
- [25] Grimmett, G., and Stirzaker, D., *Probability and random processes*, Oxford University Press, 2001.
- [26] Horn, R. A., and Johnson, C. R., *Matrix analysis*, Cambridge University Press, 1990.
- [27] Levin, D. A., and Peres, Y., *Markov chains and mixing times*, Vol. 107, American Mathematical Society, 2017.
- [28] Ross, S. M., *Introduction to probability models*, Academic Press, 2014.
- [29] Serfozo, R., *Basics of applied stochastic processes*, Springer Science & Business Media, 2009.